Kinetics of Fluorescent-Labeled Phosphatidylcholine Transfer between Nonspecific Lipid Transfer Protein and Phospholipid Vesicles†

J. Wylie Nichols

Department of Physiology, Emory University School of Medicine, Atlanta, Georgia 30322

Received September 3, 1987; Revised Manuscript Received November 18, 1987

ABSTRACT: Recently, rat liver nonspecific lipid transfer protein (nsLTP) was shown to form a fluorescent complex when allowed to equilibrate with self-quenching vesicles prepared from the fluorescent phospholipid 1-palmitoyl-2-[12-[(7-nitro-2,1,3-benzoxadiazol-4-yl)amino]dodecanoyl]phosphatidylcholine (P-C_{12}-NBD-PC) [Nichols, J. W. (1987) *J. Biol. Chem. 262*, 14172–14177]. Investigation of the mechanism of complex formation was continued by studying the kinetics of transfer of P-C_{12}-NBD-PC between nsLTP and phospholipid vesicles using a transfer assay based on resonance energy transfer between P-C_{12}-NBD-PC and *N*-(lissamine rhodamine B sulfonyl)dioleoylphosphatidylethanolamine. The principles of mass action kinetics (which predict initial lipid transfer rates as a function of protein and vesicle concentration) were used to derive equations for two distinct mechanisms: lipid transfer by the diffusion of monomers through the aqueous phase and lipid transfer during nsLTP–membrane collisions. The results of these kinetic studies indicated that the model for neither mechanism alone adequately predicted the initial rates of formation and dissolution of the P-C_{12}-NBD-PC–nsLTP complex. The initial rate kinetics for both processes were predicted best by a model in which monomer diffusion and collision-dependent transfer occur simultaneously. These data support the hypothesis that the phospholipid–nsLTP complex functions as an intermediate in the transfer of phospholipids between membranes.

Nonspecific lipid transfer protein (nsLTP)[1] stimulates the transfer of a wide range of lipids between membranes (Bloj & Zilversmit, 1977, 1981). Recently, nsLTP was shown to form a water-soluble phospholipid–nsLTP complex when allowed to equilibrate with bilayer vesicles prepared from fluorescent-labeled phospholipid, P-C_{12}-NBD-PC (Nichols, 1987a). Prior to this observation, attempts to demonstrate a phospholipid–nsLTP complex using radiolabeled phospholipids and traditional separation techniques failed (Crain & Zilversmit, 1980; Van Amerongen et al., 1985), and as a result, nsLTP was proposed to function by mechanisms not involving the direct binding of phospholipids. For example, nsLTP has been proposed to function by the formation of a ternary complex between nsLTP and the donor and acceptor membranes which would facilitate the rapid intermembrane transfer of lipids (Van Amerongen et al., 1985; Altamura & Landriscina, 1986; Megli et al., 1986). Alternatively, nsLTP has been proposed to bind to membranes and increase the rate of lipid dissociation into the water phase (Thompson, 1982; Nichols & Pagano, 1983). The demonstration that nsLTP binds phospholipids suggests that the resulting phospholipid–nsLTP complex may mediate the intermembrane transfer. The observation that the thiol reagent mersalyl blocks both nsLTP binding of phospholipids (Nichols, 1987a) and its ability to stimulate intermembrane phospholipid transfer (Van Amerongen et al., 1985; Megli et al., 1986) lends further support to this hypothesis.

The aim of this paper is to study kinetically the mechanism of transfer of phospholipids from vesicles to nsLTP and from nsLTP to vesicles. These two processes can be considered the half-reactions for intermembrane phospholipid transfer mediated by the phospholipid–nsLTP complex. Resonance energy transfer between P-C_{12}-NBD-PC and *N*-Rh-PE (Nichols & Pagano, 1982, 1983) was used to study the kinetics of transfer of P-C_{12}-NBD-PC from P-C_{12}-NBD-PC–nsLTP complexes to vesicles containing *N*-Rh-PE and vice versa. The principles of mass action kinetics were used to derive equations which predict initial lipid transfer rates as a function of protein and vesicle concentration for two distinct mechanisms of transfer: (1) lipid transfers by the diffusion of monomers through the aqueous phase; (2) lipid transfers during nsLTP–membrane collisions. The results of these kinetic studies indicated that the model for neither mechanism alone adequately predicted the initial rates for both formation and dissolution of the complex. The initial rate kinetics were predicted best for both cases by a model in which monomer diffusion and collision-dependent transfer occur simultaneously. These data support the hypothesis that the phospholipid–nsLTP complex mediates the transfer of phospholipids between membranes. A preliminary report of the work has appeared elsewhere (Nichols, 1987b).

Experimental Procedures

Materials and Routine Procedures. Dioleoylphosphatidylcholine (DOPC) and P-C_{12}-NBD-PC were purchased from Avanti Biochemical Corp. P-C_{12}-NBD-PE was prepared from P-C_{12}-NBD-PC by using phospholipase D (Comfurius & Zwaal, 1977). *N*-Rh-PE was synthesized and purified as previously described (Struck et al., 1981). Phospholipids were stored at −20 °C, periodically monitored for purity by thin-layer chromatography, and repurified when necessary. Phospholipid concentrations were determined by

† This study was supported by U.S. Public Health Service Grant GM 32342 and a grant-in-aid from the American Heart Association, Georgia Affiliate.

[1] Abbreviations: nsLTP, nonspecific lipid transfer protein; P-C_{12}-NBD-PC, 1-palmitoyl-2-[12-[(7-nitro-2,1,3-benzoxadiazol-4-yl)amino]-dodecanoyl]phosphatidylcholine; P-C_{12}-NBD-PE, 1-palmitoyl-2-[12-[(7-nitro-2,1,3-benzoxadiazol-4-yl)amino]dodecanoyl]phosphatidylethanolamine; *N*-Rh-PE, *N*-(lissamine rhodamine B sulfonyl)dioleoylphosphatidylethanolamine; DOPC, dioleoylphosphatidylcholine; HBS, HEPES-buffered saline, 0.9% NaCl in 10 mM 4-(2-hydroxyethyl)-1-piperazineethanesulfonic acid (HEPES), pH 7.4.

0006-2960/88/0427-1889$01.50/0

a lipid phosphorus assay (Ames & Dubin, 1960). Protein was assayed with fluorescamine (Roche Diagnostics).

Vesicle Preparation. Lipids were mixed in desired proportions and their storage solvents removed by evaporation under nitrogen followed by a minimum of 4 h of vacuum desiccation. Vesicles were prepared by ethanol injection (Kremer et al., 1977) as follows. Dried phospholipids were dissolved in ethanol, injected into HBS at room temperature, and dialyzed against 4 L of HBS overnight at 4 °C. Ethanol never exceeded 5% of HBS by volume, and the phospholipid concentration in ethanol never exceeded 20 mM. The resulting vesicles were used on the day following injection.

Purification of Nonspecific Lipid Transfer Protein. nsLTP was purified from rat liver as previously described by Poorthuis et al. (1981). Further purification was obtained by heating the protein solution for 5 min at 95 °C followed by chromatography of the active fractions on an octylagarose column (Crain & Zilversmit, 1980). The active fractions were eluted with pH 2 buffer and immediately titrated to pH 7. Purity of nsLTP was indicated by the detection with Bio-Rad silver stain of a single 12 500 molecular weight band following sodium dodecyl sulfate–polyacrylamide gel electrophoresis. Purified nsLTP was stored at 5 °C in buffer containing 5 mM sodium phosphate, 5 mM β-mercaptoethanol, and 0.04% sodium azide, pH 7.0, diluted 1:1 with glycerol. Activity of the fractions was assayed by measuring the rate of protein-stimulated transfer of P-C_{12}-NBD-PE between DOPC vesicles using a fluorescent assay based on resonance energy transfer between *N*-Rh-PE and P-C_{12}-NBD-PE (Nichols & Pagano, 1983).

Fluorescence Measurements. Fluorescence was recorded from a Perkin-Elmer MPF-44E fluorescence spectrometer. The analog output from the fluorometer was recorded on a chart recorder and simultaneously digitized and stored at 4 Hz on an IBM PC-XT. Solutions in the cuvette were mixed with a magnetic stirrer, and the temperature was controlled by a circulating water bath.

The fluorescence yields (relative fluorescence per mole) of P-C_{12}-NBD-PC bound to nsLTP and as a low mole fraction of DOPC vesicles were determined as demonstrated previously (Nichols, 1987a). The fluorescence yield in DOPC is obtained directly by measuring the fluorescence of a known amount of P-C_{12}-NBD-PC in DOPC vesicles. The fluorescence yield of P-C_{12}-NBD-PC bound to nsLTP is determined indirectly by measuring the ratio of fluorescence of P-C_{12}-NBD-PC first bound to nsLTP and then transferred to excess DOPC vesicles. The fluorescence yield of P-C_{12}-NBD-PC bound to nsLTP was used to quantify the initial concentration of P-C_{12}-NBD-PC complexes in the nsLTP to vesicle transfer experiments. The fluorescence yield of P-C_{12}-NBD-PC in DOPC vesicles was used to quantify the transfer from DOPC vesicles to nsLTP.

Measurement of P-C_{12}-NBD-PC Transfer from nsLTP to Vesicles. The method used for measuring P-C_{12}-NBD-PC transfer from nsLTP to vesicles is illustrated in Figure 1A. This technique has been presented in detail previously (Nichols, 1987a) and is presented below in brief.

In the first step, P-C_{12}-NBD-PC–nsLTP complexes are formed by incubation of self-quenching P-C_{12}-NBD-PC vesicles with nsLTP. The addition of nsLTP to the self-quenching vesicles results in a large increase in fluorescence as P-C_{12}-NBD-PC molecules bind to nsLTP (Nichols, 1987a). These P-C_{12}-NBD-PC–nsLTP complexes in equilibrium with P-C_{12}-NBD-PC self-quenching vesicles are used as donors to measure the transfer of P-C_{12}-NBD-PC from nsLTP to *N*-Rh-PE-containing DOPC vesicles. *N*-Rh-PE is a resonance

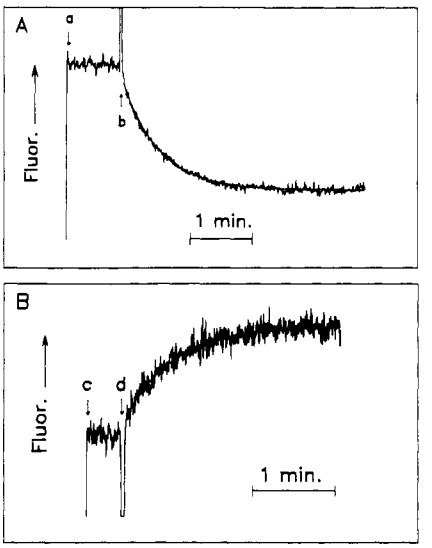

FIGURE 1: Fluorescence measurement of P-C_{12}-NBD-PC transfer between nsLTP and DOPC vesicles. (A) Recording of P-C_{12}-NBD-PC fluorescence change upon addition of *N*-Rh-PE–DOPC vesicles to a mixture of P-C_{12}-NBD-PC and nsLTP. At "a", the fluorescence of a mixture of P-C_{12}-NBD-PC (0.18 μM) and nsLTP (0.17 μM) is recorded. Concentration of P-C_{12}-NBD-PC bound to nsLTP is 21 nM. At "b", *N*-Rh-PE–DOPC vesicles (5:95 mol %, 3.3 μM total phospholipid concentration) are added, and the decrease in fluorescence is recorded. (B) Recording of P-C_{12}-NBD-PC fluorescence change upon addition of nsLTP to P-C_{12}-NBD-PC–*N*-Rh-PE–DOPC vesicles. At "c", the P-C_{12}-NBD-PC fluorescence of P-C_{12}-NBD-PC–*N*-Rh-PE–DOPC (5:5:90 mol %, 6.7 μM total phospholipid concentration) is recorded. At "d", 533 nM nsLTP were added, and the increase in fluorescence was recorded. The smooth solid lines are theoretical projections of single-exponential functions using parameters obtained from a nonlinear least-squares fit to the data. Fluorescence was recorded at excitation 475 nm, 4-nm slit width, and emission 530 nm, 4-nm slit width, at 25 °C.

energy quencher of P-C_{12}-NBD-PC (Nichols & Pagano, 1982), such that the addition of *N*-Rh-PE–DOPC vesicles to the P-C_{12}-NBD-PC–nsLTP complexes results in a decrease in fluorescence as the P-C_{12}-NBD-PC moves from nsLTP to the quenching environment of the vesicles. The transfer of P-C_{12}-NBD-PC from the self-quenching vesicles is not detected since it involves the transfer of the fluorophore from one quenching environment to another. The self-quenching vesicles may influence the kinetics of transfer and have been treated accordingly in the theoretical model.

For all experiments performed, the quenching rate of P-C_{12}-NBD-PC fluorescence could be simulated by a single-exponential decay process (see smooth solid line in Figure 1A). After correction for the spillover of *N*-Rh-PE fluorescence emitted at NBD excitation and emission wavelengths, the equilibrium value in Figure 1A indicates that essentially all of the P-C_{12}-NBD-PC initially bound to nsLTP has been transferred to and quenched by the *N*-Rh-PE–DOPC vesicles. Thus, the initial rate of transfer (R) is a product of the single-exponential rate constant and the initial concentration of P-C_{12}-NBD-PC bound to nsLTP.

Measurement of P-C_{12}-NBD-PC Transfer from Vesicles to nsLTP. The transfer of P-C_{12}-NBD-PC from vesicles to nsLTP is determined from the rate of increase in fluorescence as P-C_{12}-NBD-PC moves from the quenching environment of *N*-Rh-PE–DOPC vesicles to a nonquenching binding site on the nsLTP molecule (Figure 1B). In all cases, the fluorescence increased as a single-exponential function (see smooth solid line in Figure 1B). The amount of P-C_{12}-NBD-PC transferred at equilibrium was calculated from the P-C_{12}-NBD-PC fluorescence yield when bound to nsLTP, and thus the initial

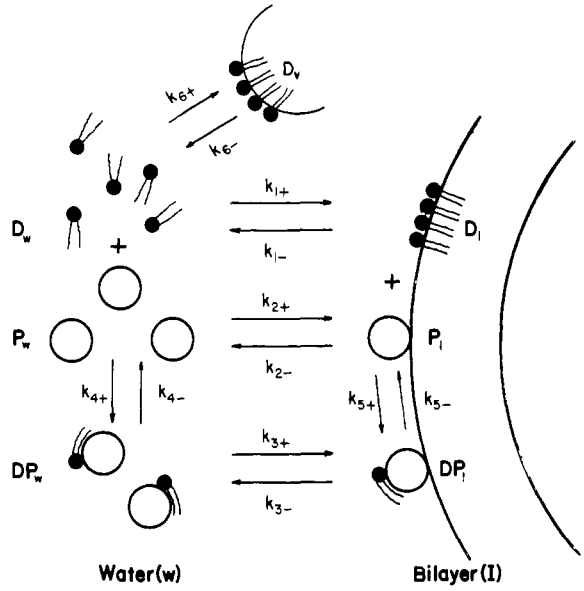

FIGURE 2: Schematic diagram of nsLTP, P-C_{12}-NBD-PC, and vesicle interactions and definition of rate constants. $[D]_w$, $[P]_w$, and $[DP]_w$ refer respectively to the bulk solution concentrations of P-C_{12}-NBD-PC, nsLTP, and P-C_{12}-NBD-PC–nsLTP complex dissolved in the water phase. $[D]_I$, $[L]_I$, $[P]_I$, and $[DP]_I$ refer respectively to the bulk solution concentrations of P-C_{12}-NBD-PC, total phospholipid, nsLTP, and P-C_{12}-NBD-PC–nsLTP complex on the external surface of the vesicle. $[D]_v$ refers to the bulk solution concentration of P-C_{12}-NBD-PC on the external surface of self-quenching vesicles. s is the monolayer surface area per phospholipid molecule.

rate was the product of the single-exponential rate constant and the concentration of P-C_{12}-NBD-PC bound to nsLTP at equilibrium.

Data Analysis. The best fit of parameters for the single-exponential curves and the theoretical transfer models was calculated on an IBM-PC-XT using a PASCAL program for the least-squares estimation of nonlinear parameters based on the Marquardt algorithm (Marquardt, 1963).

THEORY

There are two fundamentally distinct mechanisms for the transfer of lipids between nsLTP and membranes: (1) lipid transfer occurs by the diffusion of monomers through the aqueous phase, and (2) lipid transfer is dependent upon nsLTP–membrane collision. Figure 2 illustrates the reaction pathway for both mechanisms. Reactions 1 and 4 describe the monomer diffusion pathway, and reactions 2, 3, and 5 describe the collision-dependent pathway. All six reactions are necessary to describe the transfer if both mechanisms occur simultaneously.

The rate equations for lipid and protein interactions with membranes are written by assuming that the rate at which a lipid or protein molecule dissociates from the surface of a membrane is proportional to its surface concentration and that the association rate is proportional to the product of its concentration in solution and the external surface area of the membrane (Nakagawa, 1974; Thilo, 1977; Nichols & Pagano, 1981, 1982; Ferrell et al., 1985). The rate of reaction of protein and lipid on the surface of the membrane is proportional to the product of the membrane concentration of protein and lipid times the total external surface of the membrane. These general principles can be used to derive initial rate equations that predict the transfer kinetics of a lipid probe from nsLTP to vesicles and vice versa for the monomer diffusion model, the collision-dependent model, and the combination of both.

The rate constants and abbreviations of terms used in the following derivations are illustrated schematically in Figure 2 and defined in the legend.

Initial Transfer Rate of P-C_{12}-NBD-PC from nsLTP to Vesicles. (A) Collision-Dependent Model. During the initial transfer of P-C_{12}-NBD-PC from nsLTP to vesicles, its concentration in the vesicles ($[D]_I$) is assumed to be zero. According to the collision-dependent model, the initial rate of transfer of P-C_{12}-NBD-PC from nsLTP to vesicles occurs via reaction 5 and is predicted by

$$R_{coll} = k_{5-}[DP]_I \tag{1}$$

Previous experiments have demonstrated that nsLTP has a low binding affinity for vesicles (Nichols, 1987a); thus, the concentration of nsLTP bound to vesicles ($[P]_I$) will be a small fraction of the total protein, and the ternary complex of P-C_{12}-NBD-PC–nsLTP bound to vesicles ($[DP]_I$) will be an even smaller fraction. It is therefore reasonable to assume that $[DP]_I$ will reach a steady-state concentration rapidly and remain constant during the initial transfer rate measurements. Thus

$$d[DP]_I/dt = k_{3+}[DP]_w s[L]_I - k_{3-}[DP]_I - k_{5-}[DP]_I = 0 \tag{2}$$

Solving for $[DP]_I$

$$[DP]_I = \frac{k_{3+}[DP]_w s[L]_I}{k_{3-} + k_{5-}} \tag{3}$$

Since the amount of phospholipid residing in the outer leaflet of the vesicles ($[L]_I$) is a constant fraction (f) of the total ($[L]_T$)

$$[L]_I = f[L]_T \tag{4}$$

When eq 3 and 4 are substituted into eq 1, the initial rate of collision-dependent probe transfer from nsLTP to vesicles is predicted by

$$R_{coll} = \frac{k_{5-}k_{3+}sf[DP]_w[L]_T}{k_{3-} + k_{5-}} \tag{5}$$

(B) Monomer Diffusion Model. The initial rate of P-C_{12}-NBD-PC transfer from nsLTP to vesicles occurs via reaction 1 and is predicted to be

$$R_{md} = k_{1+}[D]_w s[L]_I \tag{6}$$

Modeling of the monomer diffusion mechanism is complicated by the lack of a direct measure of the probe free monomer concentration. This concentration is predicted from the steady-state distribution immediately following the addition of excess vesicles to the equilibrated mixture of P-C_{12}-NBD-PC and nsLTP. Since the steady-state concentration will depend to some extent on the concentration of P-C_{12}-NBD-PC in the form of self-quenching vesicles, the contribution of P-C_{12}-NBD-PC self-quenching vesicles to the steady-state probe free monomer concentration (reaction 6) will be included in the derivation (see Figure 2). Upon addition of excess DOPC vesicles, the probe free monomer concentration is assumed to reach a steady-state equilibrium where

$$\frac{d[D]_v}{dt} + \frac{d[DP]_w}{dt} + \frac{d[D]_I}{dt} = 0 \tag{7}$$

The corresponding initial rate equations are

$$d[D]_v/dt = k_{6+}[D]_w s[D]_v - k_{6-}[D]_v \tag{8}$$

$$d[DP]_w/dt = k_{4+}[D]_w[P]_w - k_{4-}[DP]_w \tag{9}$$

$$d[D]_I/dt = k_{1+}[D]_w s[L]_I \tag{10}$$

such that

$$[D]_w = \frac{k_{4-}[DP]_w + k_{6-}[D]_v}{k_{4+}[P]_w + k_{1+}s[L]_I + k_{6+}s[D]_v} \quad (11)$$

The molar ratios of the P-C_{12}-NBD-PC–nsLTP complexes to unbound nsLTP ($X_{DP/P}$) and to P-C_{12}-NBD-PC remaining as self-quenching vesicles ($X_{DP/V}$) can be calculated (see Experimental Procedures) and are defined as

$$X_{DP/P} = [DP]_w/[P]_w \quad (12)$$

$$X_{DP/V} = [DP]_w/[D]_v \quad (13)$$

The rate equation for probe transfer from nsLTP to vesicles according to the monomer diffusion (md) model is obtained by substituting eq 4, 11, 12, and 13 into eq 6:

$$R_{md} = [DP]_w[L]_T/\{[(k_{4+}/X_{DP/P} + k_{6+}s/X_{DP/V}) \times [DP]_w/k_{1+}sf(k_{4-} + k_{6-}/X_{DP/V})] + [[L]_T/(k_{4-} + k_{6-}/X_{DP/V})]\} \quad (14)$$

Combination of Collision-Dependent and Monomer Diffusion Models. If both collision-dependent and the monomer diffusion pathways are involved in probe transfer from nsLTP to vesicles, the initial transfer occurs via reactions 1 and 5 and is predicted by the sum of the two:

$$R_{comb} = R_{md} + R_{coll} \quad (15)$$

Initial Transfer Rate of P-C_{12}-NBD-PC from Vesicles to nsLTP. (A) Collision-Dependent Model. During the initial transfer of P-C_{12}-NBD-PC from vesicles to nsLTP, the concentration of P-C_{12}-NBD-PC–nsLTP complex ($[DP]_w$) is zero. Thus, according to the collision-dependent model

$$R_{coll} = k_{3-}[DP]_I \quad (16)$$

Because of the small size of $[P]_I$ and $[DP]_I$ relative to $[P]_w$, as discussed above, these compartments are assumed to reach a constant steady-state concentration rapidly relative to the rate of initial transfer, and

$$[P]_w \approx [P]_T \quad (17)$$

$$d[P]_I/dt = k_{2+}[P]_T s[L]_I + k_{5-}[DP]_I - k_{2-}[P]_I - k_{5+}[P]_I[D]_I/[L]_I = 0 \quad (18)$$

$$d[DP]_I/dt = k_{5+}[P]_I[D]_I/[L]_I - k_{5-}[DP]_I - k_{3-}[DP]_I = 0 \quad (19)$$

The amount of P-C_{12}-NBD-PC in the outer leaflet of the bilayer is a constant fraction (f) of the total P-C_{12}-NBD-PC and is similar to that of the total phospholipid (Nichols & Pagano, 1982). Since the rate of transbilayer movement of phospholipids is slow

$$[L]_I = f[L]_T \quad \text{and} \quad [D]_I = f[D]_T \quad (20)$$

The mole fraction of P-C_{12}-NBD-PC in the vesicles ($X_{D/L}$) is thus

$$X_{D/L} = [D]_T/[L]_T = [D]_I/[L_I] \quad (21)$$

The steady-state concentration of $[DP]_I$ is obtained from the simultaneous solution of eq 18 and 19. This relationship, and eq 20 and 21, is substituted into eq 16 to give the initial rate equation predicted by the collision-dependent model:

$$R_{coll} = \frac{k_{3-}k_{5+}k_{2+}sf[P]_T[D]_T}{k_{3-}k_{2-} + k_{3-}k_{5+}X_{D/L} + k_{5-}k_{2-}} \quad (22)$$

(B) Monomer Diffusion Model. According to the monomer diffusion model

$$R_{md} = k_{4+}[D]_w[P]_w \quad (23)$$

Assuming a steady-state concentration of $[D]_w$

$$d[D]_w/dt = k_{1-}[D]_I - k_{1+}[D]_w s[L]_I - k_{4+}[D]_w[P]_w = 0 \quad (24)$$

Thus

$$[D]_w = \frac{k_{1-}[D]_I}{k_{1+}s[L]_I + k_{4+}[P]_w} \quad (25)$$

Substitution of eq 17, 20, 21, and 25 into eq 23 gives the initial rate equation predicted by the monomer diffusion model:

$$R_{md} = \frac{[P]_T[D]_T}{[P]_T/fk_{1-} + k_{1+}s[D]_T/k_{4+}k_{1-}X_{D/L}} \quad (26)$$

Combination of Collision-Dependent and Monomer Diffusion Models. If both collision-dependent and monomer diffusion pathways are involved in P-C_{12}-NBD-PC transfer from vesicles to nsLTP, the initial rate is predicted by the sum of the two:

$$R_{comb} = R_{coll} + R_{md} \quad (27)$$

Results and Discussion

Test of Kinetic Models for P-C_{12}-NBD-PC Transfer from nsLTP to Vesicles. The schematic drawing in Figure 2 for simplicity presents a one-to-one stoichiometry of P-C_{12}-NBD-PC binding to nsLTP. However, the stoichiometry of the P-C_{12}-NBD-PC–nsLTP complex is not known. The observation in Figure 1 that the rates of P-C_{12}-NBD-PC dissociation from and association with nsLTP can be described by single-exponential functions indicates that whatever the stoichiometry is, all of the bound molecules exist in a single kinetic pool. In other words, all of the nsLTP-bound P-C_{12}-NBD-PC dissociates and associates at the same rate. Therefore, the experimental data testing the kinetic models are presented as a function of the solution concentration of P-C_{12}-NBD-PC bound to nsLTP ($[DP]_w$), and the relevant kinetic constants are expressed as the molar solution concentration of P-C_{12}-NBD-PC bound to nsLTP.

In order to distinguish which of the three kinetic models is the best predictor of the initial rates of P-C_{12}-NBD-PC transfer from nsLTP to vesicles, the initial transfer rates have been measured and plotted for various concentrations of nsLTP-bound P-C_{12}-NBD-PC and *N*-Rh-PE–DOPC vesicles (Figures 3 and 4). In Figure 3, the initial transfer rates are plotted (symbols) versus the concentration of nsLTP-bound P-C_{12}-NBD-PC at three different concentrations of vesicles, and in Figure 4, initial rates are plotted (symbols) versus vesicle concentrations at a constant concentration of nsLTP-bound P-C_{12}-NBD-PC. The data points from both plots (23 data points) were used to estimate the parameters for the three models using a nonlinear least-squares fitting program with two independent variables. The best fits of the parameters for the three models are presented in Table I. These parameters were then used to project the theoretical curves for each model and are presented in Figures 3 and 4 (dotted line, collision dependent; dashed line, monomer diffusion; solid line, combined). It is apparent from the comparison of the data points with the theoretical plots that the collision-dependent model alone is a poor predictor of the initial rates. The monomer diffusion model gives a reasonably close fit to the data. However, the smallest variance, indicating the best fit (Table I), is obtained for the combined model. One might expect that the addition of a term to the monomer diffusion model would increase the goodness of fit. An F_χ test can be used to test

Table I: Parameters for the Nonlinear Least-Squares Fit to Theoretical Models: P-C_{12}-NBD-PC Transfer from nsLTP to Vesicles (25 °C)

model[a]	general form[b] of eq	variance[c]	$P_1 \pm$ SD (s)	$P_2 \pm$ SD (s)	$P_3 \pm$ SD ($M^{-1}\cdot s^{-1}$)
collision dependent	$y = P_3x_1x_2$	1.51×10^{-2}			$(6.69 \times 10^3) \pm (0.47 \times 10^3)$
monomer diffusion	$y = x_1x_2/(P_1x_1 + P_2x_2)$	7.01×10^{-4}	7290 ± 260	6.51 ± 0.49	
combined	$y = x_1x_2/(P_1x_1 + P_2x_2) + P_3x_1x_2$	3.68×10^{-4}	9810 ± 770	5.96 ± 0.50	$(1.30 \times 10^3) \pm (0.30 \times 10^3)$

[a] See Theory for derivation of models. [b] The constants and variables are defined as follows: $x_1 = [DP]_w$; $x_2 = [L]_T$; $y = R$; $P_1 = (k_{4+}/X_{DP/P} + k_{6+}s/X_{DP/V})/[k_{1+}sf(k_{4-} + k_{6-}/X_{DP/V})] \approx k_{4+}/k_{1+}sfk_{4-}X_{DP/P}$; $P_2 = 1/(k_{4-} + k_{6-}/X_{DP/V}) \approx 1/k_{4-}$; $P_3 = k_{5-}k_{3+}sf/(k_{3-} + k_{5-})$. [c] Twenty-three experimental data points. Variance = $\{\sum[y(\text{measured}) - y(\text{theoretical})]^2\}/(N - n - 1)$. N = number of data points, n = number of parameters.

Table II: Parameters for the Nonlinear Least-Squares Fit to Theoretical Models: P-C_{12}-NBD-PC Transfer from Vesicles to nsLTP (25 °C)

model[a]	general form[b] of eq	variance[c]	$P_1 \pm$ SD (s)	$P_2 \pm$ SD (s)	$P_3 \pm$ SD ($M^{-1}\cdot s^{-1}$)
collision dependent	$y = P_3x_1x_2$	1.20×10^{-3}			$(8.19 \times 10^2) \pm (0.34 \times 10^2)$
monomer diffusion	$y = x_1x_2/(P_1x_1 + P_2x_2)$	3.43×10^{-4}	2450 ± 150	509 ± 55	
combined	$y = x_1x_2/(P_1x_1 + P_2x_2) + P_3x_1x_2$	1.69×10^{-4}	4450 ± 690	521 ± 82	$(2.97 \times 10^2) \pm (0.57 \times 10^2)$

[a] See Theory for derivation of models. [b] The constants and variables are defined as follows: $x_1 = [P]_T$; $x_2 = [D]_T$; $y = R$; $P_1 = 1/fk_{1-}$; $P_2 = k_{1+}s/k_{4+}k_{1-}X_{D/L}$; $P_3 = k_{3-}k_{5+}k_{2+}sf/(k_{3-}k_{2-} + k_{3-}k_{5+}X_{D/L} + k_{5-}k_{2-})$. [c] Twenty-six experimental data points. See footnote *c* in legend to Table I.

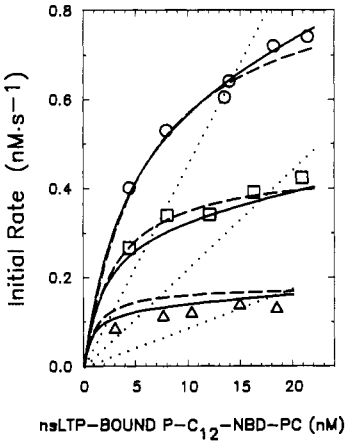

FIGURE 3: Plot of initial rate of P-C_{12}-NBD-PC transfer from nsLTP to vesicles versus the initial concentration of P-C_{12}-NBD-PC–nsLTP complexes. Experiments were performed as illustrated in Figure 1A, at 25 °C. Symbols represent the measured initial rates as the concentrations of P-C_{12}-NBD-PC–nsLTP complexes were varied for three concentrations of *N*-Rh-PE–DOPC vesicles [(○) 6.7 μM; (□) 3.3 μM; (△) 1.3 μM total phospholipid concentration]. Lines were generated from best-fit parameters estimated for the three theoretical models presented in Table I [(···) collision-dependent model; (- - -) monomer diffusion model; (—) combined model].

whether the added term significantly improves the value of the variance (Bevington, 1969). F_χ is defined as

$$F_\chi = \frac{\chi^2(n-1) - \chi^2(n)}{\chi^2(n)/(N-n-1)}$$

where N is the number of data points and n is the number of terms. This statistic follows the F distribution with 1 degree of freedom and can be used to test the null hypothesis that the coefficient of the added term is equal to zero (i.e., the new term does not improve the goodness of fit). This test when applied to the addition of the single term in the collision-dependent model to the monomer diffusion model rejects the null hypothesis with a greater than 99.9% probability. Thus, the combined model gives a significant improvement in the goodness of fit over the monomer diffusion model alone. We conclude from this analysis that both pathways are involved in the transfer of P-C_{12}-NBD-PC from nsLTP to vesicles.

To illustrate the relative contributions of the monomer diffusion and collision-dependent pathways, the magnitude of each pathway was calculated for the highest concentrations of nsLTP and vesicles used in these experiments (20 nM P-C_{12}-NBD-PC–nsLTP and 6670 nM *N*-Rh-PE–DOPC):

$R_{md} = 0.57\ nM\cdot s^{-1}$ and $R_{coll} = 0.17\ nM\cdot s^{-1}$

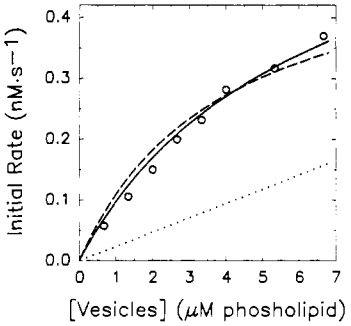

FIGURE 4: Plot of initial rate of P-C_{12}-NBD-PC transfer from nsLTP to vesicles versus concentration of vesicles. Experiments were performed as illustrated in Figure 1A at 25 °C. Symbols represent the measured initial rates as the concentration of *N*-Rh-PE–DOPC vesicles was varied. The concentration of P-C_{12}-NBD-PC–nsLTP remained constant at 3.5 nM. Lines were generated from best-fit parameters estimated for the three theoretical models presented in Table I [(···) collision-dependent model; (- - -) monomer diffusion model; (—) combined model].

At these concentrations of nsLTP (nsLTP total concentration = 0.2 μM) and vesicles, the amount of transfer via the collision-dependent reaction is 23% of the total. However, at this concentration of vesicles, the rate of transfer through the monomer diffusion pathway has saturated and will not increase significantly with higher concentrations of vesicles, whereas the rate of transfer through the collision-dependent pathway will continue to increase as a linear function of vesicles. At higher concentrations of vesicles, the collision-dependent pathway would be expected to predominate. Limitations on the rate of mixing (~2–3 s) and the response time of the Perkin-Elmer fluorometer (0.3 s) prohibited the measurement of the faster initial transfer rates that occur with higher concentrations of nsLTP and vesicles.

Test of Kinetic Models for P-C_{12}-NBD-PC Transfer from Vesicles to nsLTP. The initial transfer rate of P-C_{12}-NBD-PC from vesicles to nsLTP (see Experimental Procedures) was measured for different nsLTP and vesicle concentrations in order to determine which of the three kinetic models was the best predictor of the results. In Figure 5, the initial rates are plotted versus the concentration of P-C_{12}-NBD-PC contained as 5 mol % in DOPC vesicles for two different concentrations of nsLTP [(A) [nsLTP] = 133 nM; (B) [nsLTP] = 267 nM]. In Figure 6, the initial rates are plotted versus nsLTP concentration at two different concentrations of P-C_{12}-NBD-PC [(A) [P-C_{12}-NBD-PC] = 333 nM; (B) [P-C_{12}-NBD-PC] = 667 nM]. The data from all four plots were combined (26 data points) to estimate the parameters for all three models,

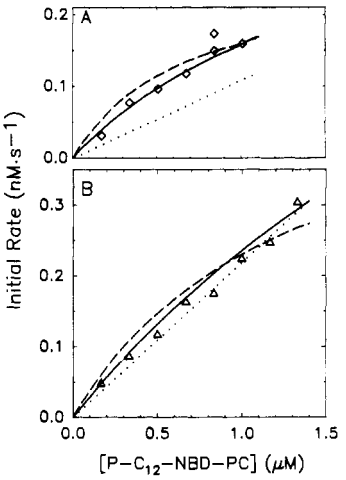

FIGURE 5: Plot of initial rates of P-C_{12}-NBD-PC transfer from vesicles to nsLTP versus concentration of P-C_{12}-NBD-PC in vesicles. Experiments were performed as illustrated in Figure 1B at 25 °C. Symbols represent initial rates measured for two concentrations of nsLTP [(□) 0.13 μM; (△) 0.27 μM nsLTP concentration] as the concentration of P-C_{12}-NBD-PC in vesicles was varied. Lines were generated from best-fit parameters estimated for the three theoretical models presented in Table II [(···) collision-dependent model; (- - -) monomer diffusion model; (—) combined model].

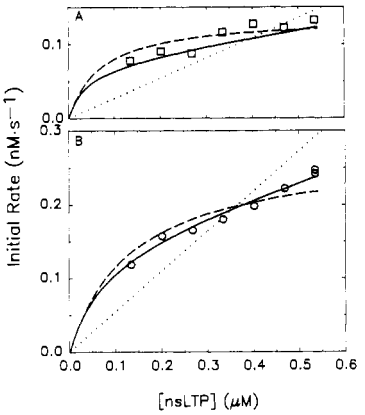

FIGURE 6: Plot of initial rate of P-C_{12}-NBD-PC transfer from vesicles to nsLTP versus concentration of nsLTP. Experiments were performed as illustrated in Figure 1B, at 25 °C. Symbols represent initial rates measured for two concentrations of P-C_{12}-NBD-PC in vesicles [(□) 0.67 μM; (○) 0.33 μM concentration of P-C_{12}-NBD-PC initially in vesicles] as nsLTP concentration was varied. Lines were generated from best-fit parameters estimated for the three theoretical models presented in Table II [(···) collision-dependent model; (- - -) monomer diffusion model; (—) combined model].

using a nonlinear least-squares fitting program with two independent variables. The best fits of the parameters are presented in Table II, and the theoretical predictions of each model are presented in Figures 5 and 6 (dotted line, collision-dependent model; dashed line, monomer diffusion model; solid line, combined model). The variance of the fits (Table II) indicates that the combined model is the best predictor of the data. The F_χ test as discussed in the previous section was used to estimate the probability that the null hypothesis—that the combination of the collision-dependent and monomer diffusion models does not significantly improve the goodness of fit—is true. This test rejects the null hypothesis with greater than 99.9% probability. Therefore, the initial rate data are best predicted by the combination of the monomer diffusion and collision-dependent pathways.

For the fastest initial transfer rate that could be measured accurately in these experiments (R_{comb} = 0.30 nM·s^{-1}, for [P-C_{12}-NBD-PC] = 1.33 μM and [nsLTP] = 267 nM), the combined model predicts that 64% of the initial rate transfer

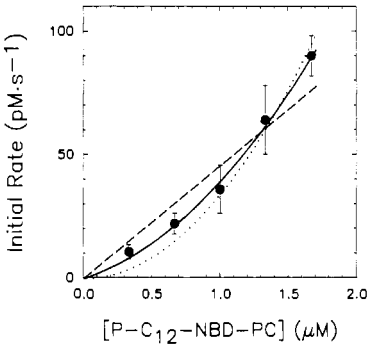

FIGURE 7: Plot of initial rate of P-C_{12}-NBD-PC transfer from vesicles to nsLTP versus concentration of P-C_{12}-NBD-PC in vesicles. Ratio of P-C_{12}-NBD-PC to nsLTP is constant. Experiments were performed as illustrated in Figure 2, at 5 °C. Closed circles represent initial rates measured as both P-C_{12}-NBD-PC and nsLTP concentrations are varied in proportion ([P-C_{12}-NBD-PC]/[nsLTP] = 5.04). Lines were generated from the best-fit parameters estimated for the three simplified theoretical models: collision-dependent model, R_{coll} = $const_1$[P-C_{12}-NBD-PC]^2, $const_1$ = 0.034, variance = 7.83 × 10^{-5}; monomer diffusion model, R_{md} = $const_2$[P-C_{12}-NBD-PC], $const_2$ = 0.046, variance = 1.18 × 10^{-4}; combined model, R_{comb} = R_{md} + R_{coll}, $const_1$ = 0.022, $const_2$ = 0.018, variance = 5.74 × 10^{-5}. Each plotted point is the average of at least three trials ± the standard deviation. Number of data points = 16.

occurs through the monomer diffusion pathway and 34% through the collision-dependent pathway.

An additional experiment (Figure 7) was performed that provides a more graphic distinction between the three theoretical transfer models. Initial transfer rates were measured at 5 °C which allowed the measurement of initial rates for higher concentrations of nsLTP and vesicles. At these higher concentrations, the collision-dependent pathway begins to predominate. Initial transfer rates were measured as the concentrations of nsLTP and P-C_{12}-NBD-PC in vesicles were increased in proportion to each other ([P-C_{12}-NBD-PC]/[nsLTP] or $[D]_T/[P]_T$ = 5.04). For this experiment, the collision-dependent model, eq 22, reduces to R_{coll} = $const_1$·$([D]_T)^2$, and the monomer diffusion model, eq 26, reduces to R_{md} = $const_2$·$([D]_T)$. Thus, the data (closed circles) presented in Figure 7 should be predicted best by a straight line if transfer occurs only by monomer diffusion and by a quadratic equation with a single term if transfer occurs only through the collision-dependent pathway. The theoretical projection for the three models (dotted line, collision dependent; dashed line, monomer diffusion; solid line, combined) illustrated that the best fit (i.e., smallest variance) is obtained from the combined model. However, in this case, as opposed to the data presented in Figures 5 and 6, the collision-dependent model gives a better fit than the monomer diffusion model, indicating that under these conditions the collision-dependent pathway is predominant. At the highest concentrations of nsLTP and P-C_{12}-NBD-PC, the combined model predicts that two-thirds of the total transfer occurs through the collision-dependent pathway (R_{coll} = 60 pM·s^{-1} and R_{md} = 30 pM·s^{-1}). The F_χ test gives a 95% certainty that the combined model is a better prediction of the initial rate data than the collision-dependent model alone and a 99.5% certainty that the combined model is a better prediction that the monomer diffusion model alone.

Extraction of Rate Constants from the Combined Model Parameters. Several meaningful rate constants, as defined in Figure 2, can be extracted from the best-fit parameters for the combined models for both directions of transfer and are presented in Table III. The dissociation rate constant for P-C_{12}-NBD-PC from DOPC vesicles (k_{1-}) can be obtained from parameter P_1 in the vesicle to nsLTP transfer experiments

Table III: Rate Constants Extracted from the Nonlinear Least-Squares Fit Parameters to the Combined Model (25 °C)[a]

experiment	k_{1-}[d] (s^{-1})	k_{4-}[e] (s^{-1})	$k_{4+}/k_{1+}s$[f]	K_1/K_4[g]
nsLTP to vesicles[b]		0.165	101	4.4
vesicles to nsLTP[c]	3.7×10^{-4}		104	4.3

[a] See Figure 2 for definition of rate constants. [b] Data and parameters presented in Figures 3 and 4 and Table I. [c] Data and parameters presented in Figures 5 and 6 and Table II. [d] Calculated from P_1 (Table II) assuming $f = 0.6$. [e] Calculated from P_2 (Table I). k_{6-} is assumed to equal k_{1-}. $X_{DP/V} = 0.114$. [f] Calculated from P_1 (Table I). k_{6+} is assumed to equal k_{1+}; $X_{DP/P} = 0.103$; $X_{DP/V} = 0.114$; $f = 0.6$; and from P_2 (Table II), $X_{D/L} = 0.05$. [g] $K_1/K_4 = k_{1+}sk_{4-}/k_{4+}k_{1-}$ was calculated from rate constants in footnotes *d*, *e*, and *f*.

(Table II). Assuming the fraction of the total phospholipid residing in the outer leaflet is 0.6, $k_{1-} = 3.7 \times 10^{-4}$ s^{-1}. An independent measurement of this rate constant determined from measurements of the spontaneous transfer of P-C_{12}-NBD-PC for vesicles of composition identical with those used in these experiments gave a value of 2.5×10^{-4} s^{-1} [see Nichols and Pagano (1982) for method]. These values for the monomer–vesicle dissociation rate constant are reasonably close and lend confidence to the parameter obtained from the vesicle to nsLTP transfer experiments.

The dissociation rate constant for P-C_{12}-NBD-PC leaving the nsLTP molecule (k_{4-}) can be obtained from parameter P_2 in the nsLTP to vesicle experiments (Table I). The dissociation rate constant from the self-quenching vesicles (k_{6-}) is of the same order of magnitude as the dissociation rate constant from DOPC vesicles (Nichols & Pagano, 1981). Since the mole fraction of nsLTP-bound P-C_{12}-NBD-PC to total P-C_{12}-NBD-PC ($X_{DP/V}$) is equal to 0.11, k_{4-} can be calculated to be 0.165 s^{-1}. The $k_{6-}/X_{DP/V}$ term is small relative to k_{4-} and results in a small (<5%) decrease of the calculated value of k_{4-}. Thus, P-C_{12}-NBD-PC dissociates from the P-C_{12}-NBD-PC–nsLTP complex into the water phase 450 times faster than it dissociates from DOPC vesicles.

Both sets of experiments provide a means of calculating the ratio of the association rate constants for P-C_{12}-NBD-PC binding to nsLTP and P-C_{12}-NBD-PC binding to DOPC vesicles. From parameter P_2 in Table II, given that the mole fraction of P-C_{12}-NBD-PC in the DOPC vesicles is 0.05, $k_{4+}/k_{1+}s = 104$. From parameter P_1 in Table I, assuming that the association rate constant for P-C_{12}-NBD-PC inserting into self-quenching vesicles is the same as that for insertion into DOPC vesicles, $k_{4+}/k_{1+}s = 101$. The similarity of the values for this ratio from the two different transfer experiments further supports the internal consistency of the method and the validity of the underlying assumptions. The ratio indicates that on a mole phospholipid per mole nsLTP basis, P-C_{12}-NBD-PC binds to nsLTP molecules 100 times faster than to DOPC vesicles.

The values for the rate constants for P-C_{12}-NBD-PC monomer–vesicle and monomer–nsLTP dissociation can be combined with the ratio of the association rate constants to give an estimate of the ratio of the affinity of a soluble P-C_{12}-NBD-PC-soluble monomer for a molecule of DOPC in the form of a bilayer vesicle versus a molecule of nsLTP ($K_1/K_4 = 4.4$).

Implications for nsLTP-Mediated Transfer of Lipids between Membranes. The goal of studying the mechanism of P-C_{12}-NBD-PC transfer between vesicles and nsLTP was to gain a better understanding of how nsLTP functions to facilitate lipid movement between membranes. Previously, nsLTP has been proposed to function by linking two membranes into a ternary complex that facilitates intermembrane lipid transfer (Van Amerongen et al., 1985; Altamura & Landriscina, 1986; Megli et al., 1986) or by transiently binding to membranes and facilitating the lipid dissociation into the water phase (Thompson, 1982; Nichols & Pagano, 1983). The demonstration of a water-soluble phospholipid–nsLTP complex (Nichols, 1987a) suggested the possibility that formation of the complex may be involved in the intermembrane transfer process. Inhibition of both lipid binding (Nichols, 1987a) and intermembrane lipid transfer (Van Amerongen et al., 1985; Megli et al., 1986; Nichols, 1987a) by the thiol reagent mersalyl suggested that they are functionally related. In order for the lipid–nsLTP complex to be an intermediate in the intermembrane transfer of lipids, nsLTP must bind lipids from the membrane surface and carry them into the water phase. nsLTP binding of lipids from the aqueous phase alone cannot increase the rate of intermembrane lipid transfer.

The evidence presented in this paper supports the conclusion that P-C_{12}-NBD-PC can be transferred between vesicles and nsLTP by a collison-dependent process. The parameters obtained from the kinetic models of P-C_{12}-NBD-PC transfer between nsLTP and vesicles can be used to illustrate the relative importance of the collision-dependent versus the monomer diffusion pathway for the intracellular transfer of phospholipids. The intracellular concentration of nsLTP and membrane lipids in liver cells can be estimated as follows. Assuming the density of liver is 1 g/cm^3, the dry weight of the cell is 40% with 10% of that being lipid; the cellular concentration of an average lipid molecule of M_r 1000 is 40 mM. The concentration of soluble nsLTP in rat liver supernatant can be calculated to range between 0.5 and 8 μM (Bloj & Zilversmit, 1977; Noland et al., 1980; Poorthuis et al., 1981; Trzaskos & Gaylor, 1983). The best-fit parameters for the combined model (Table II) can be used to calculate the rates of P-C_{12}-NBD-PC transfer from vesicles to nsLTP through each separate pathway. For a hypothetical experiment designed to reproduce these intracellular concentrations (5 μM nsLTP and 40 mM lipid) in which 5% of the membrane lipid is initially composed of P-C_{12}-NBD-PC, the combined model from Table II predicts initial rates of $R_{md} = 0.48$ nM·s^{-1} and $R_{coll} = 3 \times 10^3$ nM·s^{-1}. A similar calculation can be made for a hypothetical experiment for P-C_{12}-NBD-PC transfer from nsLTP to vesicles where initially 10% of the nsLTP is bound by P-C_{12}-NBD-PC. The parameters for the combined model in Table I predict that $R_{md} = 82$ nM·s^{-1} and $R_{coll} = 2.6 \times 10^4$ nM·s^{-1}. Thus, for these simulated intracellular conditions, the rate of P-C_{12}-NBD-PC transfer through the collision-dependent pathway is predicted to be much faster than through the monomer diffusion pathway for both directions (loading and unloading) of transfer.

Similar calculations can be used to illustrate the potential for nsLTP to increase the rate of intermembrane lipid transfer for cellular concentrations of nsLTP and membrane lipids. For the same cellular conditions assumed above, consider the hypothetical experiment where half of the membranes in the cell are instantaneously labeled with 5% P-C_{12}-NBD-PC. The initial rate of P-C_{12}-NBD-PC transfer to the rest of the cell can be calculated for a cell with and without nsLTP. Without nsLTP, P-C_{12}-NBD-PC is predicted by the monomer diffusion model for intermembrane transfer (Nichols & Pagano, 1981):

$$R_{spont} = \frac{k_{1-}[L]_I[L]_{II}X_{D/L}}{[L]_I + [L]_{II}}$$

where $[L]_I$ and $[L]_{II}$ are the membrane lipid concentrations in the donor and acceptor membranes (20 mM), respectively. k_{1-} is the dissociation rate constant for P-C_{12}-NBD-PC leaving the membrane (2.5×10^{-4} s^{-1}; see above), and $X_{D/L}$ is the mole

fraction of P-C_{12}-NBD-PC in the donor membrane (0.05). Thus

$$R_{spont} = 125 \text{ nM}\cdot\text{s}^{-1}$$

In the presence of nsLTP, since the rate of P-C_{12}-NBD-PC transfer from nsLTP to membrane was predicted above to be ~8 times faster than its transfer from the membranes to nsLTP, we can make the simplification that intermembrane transfer will be limited by the rate of lipid transfer from vesicles to nsLTP. Thus, according to the parameter P_3 from the combined model in Table II, the initial rate of nsLTP-dependent intermembrane transfer is calculated to be

$$R = 1500 \text{ nM}\cdot\text{s}^{-1}$$

For this hypothetical experiment, the concentration of nsLTP in the cell is predicted to increase the intermembrane transfer by a factor of 12. Since the spontaneous intermembrane transfer of P-C_{12}-NBD-PC is 2 times greater than dimyristoylphosphatidylcholine and 60 times greater than 1-palmitoyl-2-oleoylphosphatidylcholine (Nichols & Pagano, 1982; McLean & Phillips, 1984), the ratio of nsLTP-dependent versus spontaneous transfer for naturally occurring phospholipids may be underestimated by the P-C_{12}-NBD-PC data.

The kinetic measurements of P-C_{12}-NBD-PC transfer between nsLTP and DOPC vesicles and the predictions from intermembrane transfer demonstrate that nsLTP has the properties necessary to interact with the lipid portion of membranes and form a water-soluble phospholipid–nsLTP complex which can act as a mediator of intermembrane transfer. The rate of formation and dissociation of this complex, which determines its effectiveness as a mediator of lipid transfer via this mechanism, may also be regulated by the specific interaction with membrane proteins in the donor or target membranes. The recent demonstration that nsLTP binds to mitochondrial membrane (Megli et al., 1986) illustrates the potential for regulation of the direction and rate of nsLTP-mediated phospholipid transfer between intracellular membranes. Although the experiments presented in this paper demonstrate that nsLTP has the necessary properties to bind and carry lipids between membranes, further experiments will be required to determine the relative significance of this mechanism versus others for the intracellular movement of lipids.

REFERENCES

Altamura, N., & Landriscina, C. (1986) *Int. J. Biochem. 18*, 513–517.

Ames, B. N., & Dubin, D. T. (1960) *J. Biol. Chem. 235*, 769–775.

Bevington, P. R. (1969) *Data Reduction and Error Analysis for the Physical Sciences*, McGraw-Hill, New York.

Bloj, B., & Zilversmit, D. B. (1977) *J. Biol. Chem. 252*, 1613–1619.

Bloj, B., & Zilversmit, D. B. (1981) *Mol. Cell. Biochem. 40*, 163–172.

Comfurius, P., & Zwaal, R. F. A. (1977) *Biochim. Biophys. Acta 488*, 36–42.

Crain, R. C., & Zilversmit, D. B. (1980) *Biochemistry 19*, 1433–1439.

Ferrell, J. E., Jr., Lee, K.-J., & Huestis, W. H. (1985) *Biochemistry 24*, 2857–2864.

Kremer, J. M. H., Esker, M. W. J. v. d., Pathmamanoharan, C., & Wiersema, P. H. (1977) *Biochemistry 16*, 3932–3935.

Marquardt, D. W. (1963) *J. Soc. Ind. Appl. Math. 11*, 431–441.

McLean, L. R., & Phillips, M. C. (1984) *Biochemistry 23*, 4624–4630.

Megli, F. M., De Lisi, A., Van Amerongen, A., Wirtz, K. W. A., & Quagliariello, E. (1986) *Biochim. Biophys. Acta 861*, 463–470.

Nakagawa, T. (1974) *Colloid Polym. Sci. 252*, 56–64.

Nichols, J. W. (1985) *Biochemistry 24*, 6390–6398.

Nichols, J. W. (1987a) *J. Biol. Chem. 262*, 14172–14177.

Nichols, J. W. (1987b) *Biophys. J. 51*, 530a.

Nichols, J. W., & Pagano, R. E. (1981) *Biochemistry 20*, 2783–2789.

Nichols, J. W., & Pagano, R. E. (1982) *Biochemistry 21*, 1720–1726.

Nichols, J. W., & Pagano, R. E. (1983) *J. Biol. Chem. 258*, 5368–5371.

Noland, B. J., Arebalo, R. E., Hansbury, E., & Scallen, T. J. (1980) *J. Biol. Chem. 255*, 4282–4289.

Poorthuis, B. J. H. M., Glatz, J. F. C., Akeroyd, R., & Wirtz, K. W. A. (1981) *Biochim. Biophys. Acta 665*, 256–261.

Struck, D. K., Hoekstra, D., & Pagano, R. E. (1981) *Biochemistry 20*, 4093–4099.

Thilo, L. (1977) *Biochim. Biophys. Acta 469*, 326–334.

Thompson, T. E. (1982) *J. Am. Oil Chem. Soc. 59*, 309A.

Trzaskos, J. M., & Gaylor, J. L. (1983) *Biochim. Biophys. Acta 751*, 52–65.

Van Amerongen, A., Teerlink, T., Van Heusden, G. P. H., & Wirtz, K. W. A. (1985) *Chem. Phys. Lipids 38*, 195–204.